Erschienen in: Physica Status Solidi (RRL) - Rapid Research Letters ; 10 (2016), 4. - S. 305-309
https://dx.doi.org/10.1002/pssr.201510443

Contacting boron emitters on n-type silicon solar cells with aluminium-free silver screen-printing pastes

Susanne Fritz*, Josh Engelhardt, Stefanie Ebert, and Giso Hahn

Department of Physics, University of Konstanz, 78457 Konstanz, Germany

Keywords silicon, solar cells, boron emitters, metallization, screen-printing, aluminium-free, silver paste

* Corresponding author: e-mail susanne.fritz@uni-konstanz.de, Phone: +49 (0)7531/88-2082, Fax: +49 (0)7531/88-3895

In the production of n-type Si solar cells, B diffusion is commonly applied to form the p^+ emitter. Up to now, Ag screen-printing pastes, generally used to contact P emitters, had been incapable of reliably contact B emitters. Therefore, a small amount of Al is generally added to Ag pastes to allow for reasonable contact resistances. The addition of Al, however, results in deep metal spikes growing into the Si surface that can penetrate the emitter. Losses in open-circuit voltage are attributed to these deep metal spikes. In this investigation we demonstrate, that state-of-the-art Al-free Ag screen-printing pastes are capable to contact BBr_3-based B emitters covered with different dielectric layers and reach specific contact resistances <1 mΩ cm^2. Bifacial n-type solar cells with Al-free Ag pastes on both sides show efficiencies of up to 18.3% and series resistances <0.5 Ω cm^2.

1 Introduction Due to higher carrier lifetimes and the absence of light induced degradation, n-type silicon (Si) material shows a higher efficiency potential compared to p-type material. Therefore, different industrially relevant n-type solar cell concepts have emerged in the last years. Commonly, the p^+ layer is realized in form of a boron (B) emitter. With the use of B emitters different challenges had to be overcome. For example, different passivation layers than the ones used for phosphorous (P) emitters need to be used on B emitters, as hydrogen-rich silicon nitride (SiN_x:H) layers show insufficient passivation quality. Another challenge to be solved is metallization of B emitters by screen-printing which is the process commonly applied in industry. Older generations of standard silver (Ag) screen-printing pastes used for contacting P emitters are not capable to reliably contact B emitters. Contact resistances above 50 mΩ cm^2 are generally reported [1–4]. These high values are attributed to a lack of Ag crystals on the Si surface. For screen-printing metallization of P emitters with standard Ag pastes, surface defects at the Si/contact-interface are needed to facilitate the growth of Ag crystals [5]. These defects can exist as, e.g., crystal defects or precipitates of electrically inactive P usually present at the surface of P emitters with high P surface concentrations [6, 7]. An additional impact on the specific contact resistance is given by the different current transport mechanisms of the metal-semiconductor contact for different doping densities (field emission, thermionic field emission and thermionic emission). Lowly doped emitters with a reduced P surface concentration are therefore difficult to contact.

In the last years new Ag pastes have been developed to allow contacting of P emitters with dopant surface concentrations down to the lower 10^{20} cm^{-3} range [8].

During diffusion of B emitters often a boron-rich layer (BRL) forms at the Si surface. This layer is highly recombination active and is therefore generally removed. The resulting B emitters generally feature dopant surface concentrations below 10^{20} cm^{-3} and no precipitates of inactive B exist at the wafer surface. Therefore, Ag crystal formation on B emitters is reduced. Part of the issue was solved in 2005, when Kopecek et al. proposed to add a small amount of aluminium (Al) to the Ag screen-printing paste [1]. With the addition of Al the specific contact resistance can be reduced from >100 mΩ cm^2 to <10 mΩ cm^2. Further investigations followed to optimize paste formulation [2, 3]. Today Ag/Al screen-printing pastes allow contact

resistances of below 4 mΩ cm^2 and are commonly used to contact B emitters by screen-printing.

However, with the addition of Al the contacting issue was only partially solved. The contact formation process of Ag/Al pastes to B emitters is totally differing from the one of Ag pastes to P emitters [9]. For Al-free paste, metal oxides contained in the glass are responsible for the melting of Ag at temperatures below the melting point of Ag and the formation of Ag crystals at the Si surface [10]. In Al-containing pastes these tasks are at least to a large part undertaken by the Al. Facilitated by Al, deep metal spikes grow locally into the Si surface. With a depth of up to several µm depending on paste and firing conditions they are remarkably deeper than Ag crystals found below Ag screen-printed contacts on P emitters [10]. As B emitters generally feature a depth of around 500 nm, the spikes can be deep enough to penetrate the emitter and affect the space charge region enhancing metallization induced recombination [11]. Therefore, this spiking is made responsible for V_{oc} losses limiting cell efficiency [12, 13], and the influence of the spikes on cell characteristics is topic of ongoing research [13, 14]. Hence, screen-printed metallization exhibiting shallower Si penetration would be highly desirable and paste designers work to improve the pastes in this respect.

In 2015, Engelhardt et al. published a promising approach for B emitters diffused from SiO_x:B layers deposited by inductively coupled plasma-plasma enhanced chemical vapour deposition (ICP-PECVD) [15]. They did not change paste formulation but left the doping layer (SiO_x:B) on the wafer serving as passivation layer and used a commercially available Al-free Ag screen-printing paste to contact the emitter. With this concept specific contact resistances around 1 mΩ cm^2 have been reached on passivation layers of varying thicknesses. They attributed their results to a high defect density at the Si surface due to the presence of the doping layer.

Another successful approach to contact B emitters by a seed and plate process was presented by Kalio et al. [16]. They deposited Al-free Ag ink by aerosol jet printing and thickened the seed layer by Ag plating. Depending on the dielectric layer specific contact resistances below 5 mΩ cm^2 were reached.

In this work we show that state-of-the-art Al-free Ag pastes are capable to reliably contact BBr_3-based B emitters coated with two different dielectric layers. Contact formation of different commercially available Ag pastes is investigated by means of transfer length method (TLM) and scanning electron microscopy (SEM).

2 Experimental For the experiment two different groups of 6 inch pseudo-square n-type Cz Si wafers with a resistivity of around 5 Ω cm were used. The wafers were alkaline textured and cleaned. Then $a \approx 50$ Ω/□ B emitter was diffused in a BBr_3-based process. In the following, two groups of wafers were processed differently: wafers of group 1 received a thermal oxidation followed by a PECVD of SiN_x:H, to realize a SiO_2/SiN_x:H (7 nm/65 nm) stack. As previously discussed, SiN_x:H layers do not reasonably passivate B emitters. However, the contact formation does not fundamentally differ for different dielectric layers as analyzed in another experiment. For process simplicity therefore a simple PECVD SiN_x:H layer (75 nm) is deposited on wafers of group 2.

After that, TLM test structures with a printed finger width of 200 µm were screen-printed with three different commercially available Al-free Ag screen-printing pastes. Paste Ag1 is a paste specially developed to contact P emitters with low sheet resistance, pastes Ag2 and Ag3 are standard Ag pastes from different suppliers. In the following, contacts were fired in an IR belt furnace. For group 1, three different peak firing temperatures were used. Group 2 was fired at only one temperature.

To enable TLM for determining the specific contact resistance, TLM structures were isolated by sawing.

For analysis of the contact microstructure by means of SEM, in the following contacts were etched back in diluted hydrofluoric acid. Additionally, polished cross-sections of contacts were prepared. To allow a comparison with Al-containing pastes samples with Ag/Al contacts produced in a comparable process were prepared for SEM investigation as well. The samples were then analyzed with a Zeiss Neon40EsB SEM.

Additionally, first bifacial n-type solar cells (5 × 5 cm^2) were processed with Al-free Ag screen-printing pastes on front and back side. For the solar cells n-type Cz Si base material was used. The cells were alkaline textured on both sides and feature a homogeneous P front surface field (FSF) formed in a $POCl_3$ diffusion (60 Ω/□) and a 50 Ω/□ BBr_3-based B emitter on the back side of the cell. The FSF is passivated by 75 nm PECVD SiN_x:H whereas on the emitter side an Al_2O_3/SiN_x:H stack is used (Al_2O_3 deposited by atomic layer deposition). Front side metallization of all cells is realized with the same Ag paste (Ag3) for better comparison. For contacting the B emitter, two different Al-free Ag pastes (Ag1 and Ag3) are tested. The metallization fraction of the front and back side differed and was 6.7% and 16.3%, respectively.

3 Results Relevant parameters for wafers of group 1 and 2 are presented in Table 1.

Emitter sheet resistances R_{SH} were obtained by TLM. The B surface concentration N_B, maximum concentration N_{max} and emitter depth d_E are extracted from the emitter

Table 1 Relevant parameters of dielectric layers and emitters.

	group 1	group 2
dielectic layer	SiO_2/SiN_x	SiN_x
R_{SH} (Ω/□)	60	48
N_B (cm^{-3})	3.4×10^{19}	7.3×10^{19}
N_{max} (cm^{-3})	8.1×10^{19}	9.9×10^{19}
d_E (µm)	≈0.6	≈0.6

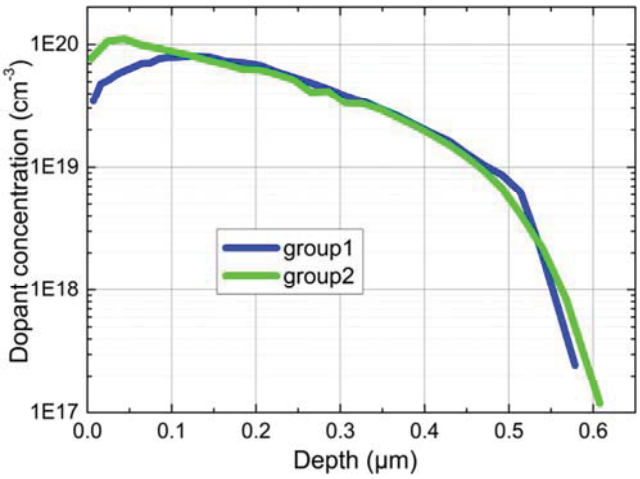

Figure 1 Emitter profiles of samples of group 1 (SiO_2/SiN_x) and group 2 (SiN_x) obtained by ECV measurement. The stronger B surface depletion of the group 2 emitter is due to the high temperature step during thermal oxidation.

profiles shown in Fig. 1, measured by electrochemical capacitance voltage measurement (ECV). Due to the additional high temperature step and out-diffusion of B from the emitter into the SiO_2 during thermal oxidation, the B emitter of group 1 shows a stronger B depletion at the surface compared to the group 2 emitter. For both emitters the B surface concentrations are 1–2 orders of magnitude below the dopant surface concentrations needed to reasonably contact P emitters with standard Ag pastes [8].

Specific contact resistances ϱ_c of the different samples measured by TLM are shown in Fig. 2. For all samples median values as well as mean values (points) for ϱ_c lie well below 10 mΩ cm^2. These values are well below specific contact resistances of Al-free Ag pastes to B emitters reported in the past. For all pastes data scattering decreases with increasing firing temperature, indicated by the boxes

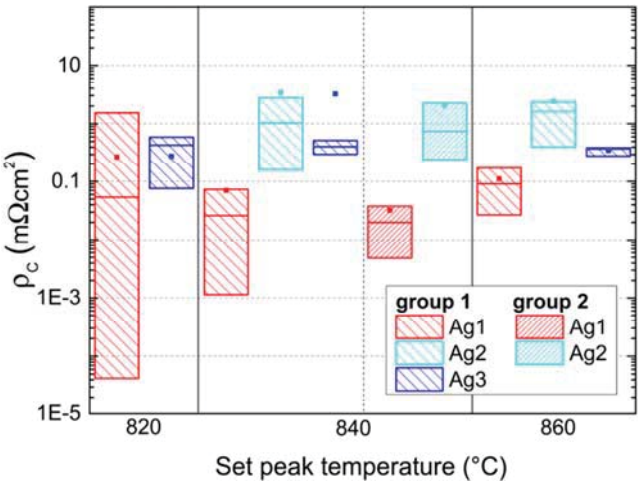

Figure 2 Specific contact resistances measured by TLM after firing at different set peak temperatures. Samples of group 1 are passivated with a SiO_2/SiN_x stack, group 2 with SiN_x.

in which 50% of the measured values are located. For paste Ag1 very low individual values are measured. They are due to the insensitivity of the TLM for very small ϱ_c values. This means that the very low values are quantitatively not reliable and just indicate a very small ϱ_c. On group 2 wafers slightly lower contact resistances are obtained compared to the values for paste Ag1 and Ag2 of group 1 fired at 840 °C. This is very likely due to the influence of differences in the emitter parameters on contact resistance [17]. Typical ϱ_c values for commercially available Al-containing Ag screen-printing pastes on wafers processed like the samples of group 2 lie between 2 mΩ cm^2 and 4 mΩ cm^2.

To compare contact formation of Al-containing with Al-free Ag screen-printing pastes, a SEM analysis was conducted. Figure 3 shows SEM micrographs where the upper images show an Al-containing contact (AgAl paste) while on the images below an Al-free contact (paste Ag2) can be seen. The images (a) and (b) show contacts etched back in diluted hydrofluoric acid. On the Si surface of paste AgAl, large AgAl crystals can be found containing Al and Si (compare with [18]). They feature diameters of more than 2 µm and appear locally distributed over the contact area. On the Si surface of paste Ag2 smaller Ag crystals can be seen that are homogeneously distributed over the contact area. Images (c)–(f) show polished cross-sections of contacts of the two pastes. The straight lines visible in the metal phase especially in (e) and (f) are scratches remaining from the polishing process. For the AgAl paste two regions can be distinguished in the contact (Fig. 3c): homogeneous regions consisting of Ag and glass, and inhomogeneous regions that contain Al (marked by dashed red circles). Large Ag crystals can be found grown into the Si solely below these Al containing regions [9]. The metal spike shown in Fig. 3e has a depth of more than 1 µm and can therefore easily penetrate into the space charge region, or even reach the base. For better visibility, the position of the former Si surface is marked by the red dashed line in the image. The Al-free contact shown in Fig. 3d, however, shows a homogeneous structure over the whole contact. The magnified image (f) shows the small Ag crystals grown into the Si. They show a depth of less than 100 nm in this case. The arrows highlight crystals that most likely contribute to the current transport, as they are separated from the bulk metal by a very thin glass layer. Depending on paste and temperature, crystals penetrating slightly deeper into the emitter can be observed.

The SEM analysis shows that contact formation of Al-free Ag pastes to B emitters completely differs from that of Al-containing pastes. The Ag crystals on the Si surface penetrate considerably less deep into the wafer and therefore the risk of shunting and degradation of the space-charge region should be reduced.

The best produced solar cell in the first solar cell experiment was metallized with paste Ag1 on the B emitter side and Ag3 on the front side of the cell. It features an efficiency of $\eta = 18.3\%$ showing that principally solar cells with B emitter can be contacted by Al-free Ag pastes on

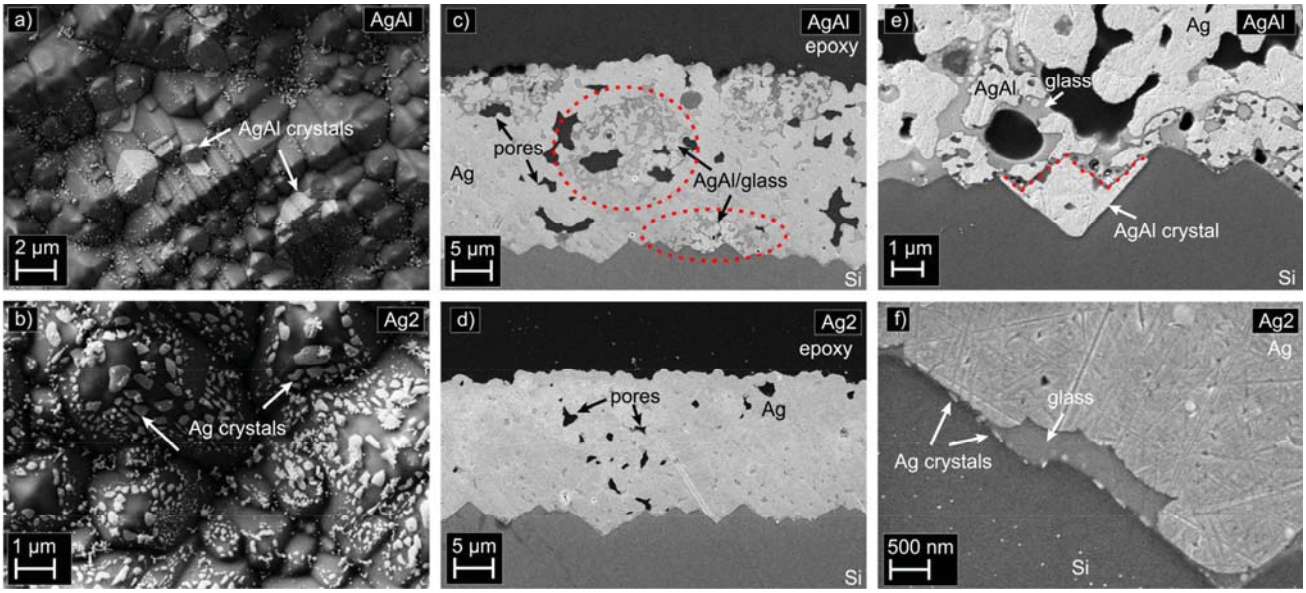

Figure 3 (a), (b) Top view SEM micrographs of contacts of AgAl paste (a) and Ag2 (b) etched back in diluted HF. (c)–(f) SEM micrographs of polished cross-sections of AgAl paste (c, e) and paste Ag2 (d, f).

both sides. The low contact resistances presented before are confirmed by the low series resistance R_{series} of 0.4 Ω cm^2 and a reasonable shunt resistance R_{shunt} of 2 kΩ cm^2 is reached. Short-circuit current density and fill fac-tor are 37.4 mA/cm^2 and 77.1%, respectively. A loss of 30 mV in open-circuit voltage V_{oc} can be observed due to metallization (difference between implied V_{oc} = 660 mV and V_{oc} = 630 mV). This is comparable with the V_{oc} loss on solar cells contacted with Al-containing pastes in the same experiment and lies in the same order of magnitude as reported in literature [12, 13]. It must be emphasized that the solar cell process and firing parameters were not optimized to the Al-free Ag paste in this first experiment.

4 Discussion The results show that state-of-the-art Al-free Ag screen-printing pastes are capable to form a reasonably good contact to B emitters formed in a BBr_3-based process through different dielectric layers. Especially, Ag pastes developed to contact lowly doped P emitters (Ag1) lead to contact resistances below 1 mΩ cm^2, but for standard Ag pastes low ϱ_c values below 10 mΩ cm^2 were presented as well. The reason for the low contact resistances can be found in the existence of Ag crystals at the silicon surface. A comparison of the contact interface with the one of Al-containing Ag pastes however, shows that deep metal spiking can be prevented by the use of Al-free pastes.

The reason for the improvement of Al-free pastes with regard to contacting B emitters may be due to different factors. In contrast to the investigation of Engelhardt et al. [15] where the doping layer was kept on the Si wafer serving as passivation layer, the dielectric layers were deposited after emitter formation. Due to the presence of B in the top Si layer and segregation of additional B into the SiO_2 layer during thermal oxidation, the dielectric layer of group 2 contains B atoms. The situation is therefore comparable as for the investigation in [15]. For the wafers of group 1, however, no SiO_2:B exists. Therefore, the explanation that a high defect density at the Si surface is only caused by the presence of the SiO_2:B doping layer cannot explain the observations.

Another explanation can be that changes in glass frit composition facilitate the growth of Ag crystals on the silicon surface. The fact that the lowest contact resistance in this investigation was obtained for paste Ag1, especially developed to contact lowly doped emitters, further supports this assumption. Modifications in actual emitters compared to emitters processed in older processes can be another explanation for the observations, e.g., the type of thermal oxidation commonly applied after BBr_3-diffusion for better removal of the boron-rich layer [19] could alter the Si surface and therefore improve the ability to contact the wafer.

First solar cells produced with Al-free pastes on B emitters show cell efficiencies of 18.3% and series resistances below 0.5 Ω cm^2, additionally demonstrating the capability of Al-free pastes to reliably contact B emitters. Despite the use of Al-free pastes on the B side of the solar cell, V_{oc} losses of around 30 mV are observed that are comparable with the loss obtained with Al-containing pastes. This could indicate that the observed V_{oc} losses cannot solely be attributed to the AgAl spikes observed for Al-containing pastes. Other mechanisms like, e.g., in-diffusion of metal from the paste or the contact into the Si induce a degradation of the emitter or space charge region and are a source of metallization induced recombination,

too. As the firing process was not optimized for the Al-free pastes, low V_{oc} and FF values could additionally be caused by the non-optimized firing conditions.

The ability to contact B emitters with Al-free Ag screen-printing pastes allows to use only one screen-printing paste on both sides of bifacial solar cells, or even more attractive for both polarities of interdigitated back contact (IBC) solar cells, reducing process complexity and processing cost. With the prevention of deep spiking and optimized firing parameters it could be possible to improve cell characteristics compared to cells contacted with Ag/Al pastes, especially the V_{oc} values.

5 Conclusion In this work we presented specific contact resistances below 1 mΩ cm^2 by contacting BBr_3-based B emitters with state-of-the-art Al-free Ag screen-printing pastes fired through two different passivation layers. It was shown that the low contact resistance can be attributed to the presence of Ag crystals at the Si/contact interface. In contrast to standard Ag/Al pastes where deep metal spikes with depth >500 nm are observed especially for higher firing temperatures, the crystals below Al-free contacts only show a shallow penetration into the silicon surface. First bifacial n-type solar cells processed with Al-free pastes on both sides show efficiencies up to 18.3% and very low series resistances of 0.4 Ω cm^2. Despite the avoidance of deep metal spiking, we still observe a 30 mV difference between implied V_{oc} and V_{oc} on cell level. This behaviour is not understood yet and subject to further investigation.

Acknowledgements Part of this work was financially supported by the German Federal Ministry for the Environment, Nature Conservation, and Nuclear Safety (FKZ 0325581). The content of this publication is the responsibility of the authors.

References

[1] R. Kopecek, T. Buck, J. Libal, R. Petres, I. Röver, K. Wambach, R. Kinderman, L. J. Geerligs, and P. Fath, in: Proc. 14th IPSEC, Shanghai, China, 2005, pp. 892–894.

[2] H. Kerp, S. Kim, R. Lago, F. Recart, I. Freire, L. Pérez, K. Albertsen, J. C. Jiméno, and A. Shaikh, in: Proc. 21st EUPVSEC, Dresden, Germany, 2006, pp. 892–894.

[3] R. Lago, L. Pérez, H. Kerp, I. Freire, I. Hoces, N. Azkona, F. Recart, and J. C. Jimeno, Prog. Photovolt.: Res. Appl. **18**, 20–27 (2010).

[4] S. Riegel, F. Mutter, T. Lauermann, B. Terheiden, and G. Hahn, Energy Procedia **21**, 14–23 (2012).

[5] S. Riegel, F. Mutter, G. Hahn, and B. Terheiden, Energy Procedia **8**, 533–539 (2011).

[6] G. Schubert, J. Horzel, R. Kopecek, and F. Huster, in: Proc. 20th EUPVSEC, Barcelona, Spain, 2005, pp. 934–937.

[7] E. Cabrera, S. Olibet, D. Rudolph, P. E. Vullum, R. Kopecek, D. Reinke, C. Herzog, D. Schwaderer, and G. Schubert, Progr. Photovolt.: Res. Appl. **23**, 367–375 (2015).

[8] V. Shanmugam, J. Cunnusamy, A. Khanna, P. K. Basu, Y. Zhang, C. Chen, A. F. Stassen, M. B. Boreland, T. Mueller, B. Hoex, and A. G. Aberle, IEEE J. Photovolt. **4**, 168–174 (2014).

[9] S. Fritz, M. König, S. Riegel, A. Herguth, M. Hörteis, and G. Hahn, IEEE J. Photovolt. **5**, 145–151 (2015).

[10] G. Schubert, F. Huster, and P. Fath, Sol. Energy Mater. Sol. Cells **90**, 3399–3406 (2006).

[11] N. Wöhrle, E. Lohmüller, J. Greulich, S. Werner, and S. Mack, Sol. Energy Mater. Sol. Cells **146**, 72–79 (2016).

[12] I. G. Romijn, B. van Aken, J. Anker, A. R. Burgers, A. Gutjahr, B. Heurtault, M. Koppes, E. Kossen, M. Lamers, D. S. Saynova, C. J. J. Tool, L. Fang, X. Jingfeng, L. Gaofei, X. Zhuo, W. Hongfang, H. Zhiyan, P. R. Venema, and H. G. Vlooswijk, in: Proc. 27th EUPVSEC, Hamburg, Germany, 2012, pp. 533–537.

[13] A. Edler, V. D. Mihailetchi, L. J. Koduvelikulathu, R. Kopecek, and R. Harney, Prog. Photovolt.: Res. Appl. **23**, 620–627 (2014).

[14] F. D. Heinz, M. Breitwieser, P. Gundel, M. König, M. Hörteis, W. Warta, and M. C. Schubert, Sol. Energy Mater Sol. Cells **131**, 105–109 (2014).

[15] J. Engelhardt, A. Frey, S. Gloger, G. Hahn, and B. Terheiden, Appl. Phys. Lett. **107**, 042102 (2015).

[16] A. Kalio, A. Richter, M. Glatthaar, and J. Wilde, Energy Procedia **38**, 745–752 (2013).

[17] E. Lohmüller, S. Werner, R. Hoenig, J. Greulich, and F. Clement, Sol. Energy Mater. Sol. Cells **142**, 2–11 (2015).

[18] S. Fritz, S. Riegel, A. Hammud, H. Deniz, and G. Hahn, IEEE J. Photovolt., DOI: 10.1109/JPHOTOV.2015.2493363 (2015).

[19] J. Libal, R. Petres, R. Kopecek, G. Hahn, K. Wambach, and P. Fath, in: Proc. 20th EUPVSEC, Barcelona, Spain, 2005, pp. 1209–1212.